

## A Novel Two-Dimensional Wind Speed and Direction Measurement Method Based on NTC

Noura SOUKAR<sup>1\*</sup>, Ayhan YAZGAN<sup>2</sup>

<sup>1</sup> ArGesim Teknoloji A.S., Çorum, Türkiye

<sup>2</sup> Electrical-Electronics Engineering Department, Graduate School of Natural and Applied Sciences, Karadeniz Technical University, Trabzon, Türkiye

\*<sup>1</sup> nsoukar@argesim.com.tr, <sup>2</sup> ayhanyazgan@ktu.edu.tr

(Geliş/Received: 28/09/2024;

Kabul/Accepted:12/03/2025)

**Abstract:** Traditional wind sensors, such as cup, hot wire, ultrasonic, and laser Doppler anemometers, often have mechanical parts that limit sensitivity, accuracy, and durability, unlike thermal flow sensors, which detect the wind by measuring the temperature variations using a heater. In addition, the methods reported in the literature have different advantages and disadvantages. In this study, different thermal flow sensor designs reported in the literature are examined and a new method based on the 2-dimensional NTC thermistor is proposed. Simulation results of the proposed method are presented. According to the results actual and calculated wind speed measurements well matched and the maximum wind speed error observed is less than %3. In addition, a simple testbed is presented for wind direction measurement.

**Key words:** Wind sensor, wind speed, wind direction, anemometer, thermal flow sensor.

### NTC Tabanlı Yeni Bir İki-Boyutlu Rüzgar Hızı ve Yönü Ölçüm Yöntemi

**Öz:** Geleneksel rüzgâr sensörleri, bir ısıtıcı kullanarak sıcaklık değişimlerini ölçerek rüzgârı algılayan termal akış sensörlerinin aksine, kupalı, ultrasonik ve lazer Doppler anemometre gibi, genellikle hassasiyet, doğruluk ve dayanıklılığı sınırlayan mekanik parçalara sahiptir. Bunların yanında, literatürde rapor edilen yöntemlerin farklı avantajları ve dezavantajları bulunmaktadır. Bu çalışmada ise, literatürde rapor edilen farklı termal akış sensörü tasarımları incelenmiş ve 2 boyutlu NTC sensörünü temel alan yeni bir yöntem önerilmiştir. Önerilen yöntemin simülasyon sonuçları sunulmuştur. Sonuçlara göre gerçek ve hesaplanan rüzgâr hızı ölçümleri iyi bir şekilde eşleşmiştir ve gözlenen maksimum rüzgar hızı hatası %3'ten azdır. Ek olarak rüzgâr yönünün tespiti için basit bir düzenek de sunulmuştur.

**Anahtar kelimeler:** Rüzgâr sensörü, rüzgar hız, rüzgar yön, anemometre, termal akış sensörleri.

### 1. Introduction

Wind sensors, also known as anemometers, are tools used to measure wind speed and direction. Typically, these sensors include mechanical components that can affect their sensitivity, accuracy, and durability. This study will examine different sensors that measure wind speed and direction through temperature changes.

Wind sensors are commonly utilized in environmental monitoring, meteorology, and energy production to measure wind speed and direction. They come in various models based on different operating principles [1]. Cup Anemometer is known as the most common wind speed sensor in meteorological stations. It consists of three or four cups rotating around a vertical axis. The number of rotations is proportional to wind speed [2]. Ultrasonic Anemometer is based on the operating principle of Ultrasonic Transmitter-Receiver converters. It works by sending a sound wave from the transmitter converter. The microprocessor then measures the time it takes for the signal to be received by the receiver converter. Ultimately, the wind speed is measured by calculating the time it takes for the sound waves to travel between the converters [3]. Laser Doppler Anemometer determines the wind speed using the Doppler effect. It operates by splitting a laser light beam into two beams when these two narrow light beams focus on a stationary object. However, when the object is moving, the returning beam's frequency changes, resulting in a differing transmitted signal. This variance in frequency, known as the Doppler shift, allows for the measurement of wind speed [4]. Hot Wire Anemometer is based on the principle of heat loss. It consists of two probes between which a thin wire is stretched. When the wire is kept at a constant temperature, as the wind blows over the hot wire, it cools down, and its resistance changes. The wire's resistance is directly proportional to the speed of the airflow [5]. Thermistor-Based Anemometer measures wind speed using PTC (Positive Temperature Coefficient) or NTC (Negative Temperature Coefficient) thermistors. As the wind blows, the thermistor cools, causing a change in its resistance. Simple structure, compact size, and fast response are the advantages of this method [6-7].

\* Corresponding author: nsoukar@argesim.com.tr. ORCID Number of authors: <sup>1</sup> 0000-0003-3876-4551, <sup>2</sup> 0000-0003-2209-2973

Recently, studies have aimed to develop a new wind sensor interface that utilizes thermal flow sensors without any mechanical components [8]. This type of sensor has three basic measurement principles: time-of-flight, hot wire, and calorimetric [6]. Using the hot wire measurement principle, wind speed is calculated by measuring the heat loss brought on by wind. It may operate in either the Constant Power (CP) or Constant Temperature Difference (CTD) modes. The heater's temperature controls the flow rate when operating in the Constant Power Mode, ensuring a steady power supply. On the other hand, the heater's power consumption in the CTD mode indicates the flow speed and maintains the heater's temperature a few degrees above the flow temperature [9-10]. Low-cost silicon sensors for mass flow measurement were also proposed [11]. The calorimetric measurement principle detects variations in heat gradients caused by wind using a central heating source and surrounding thermal sensors. With this information, the wind's direction and speed were calculated and reported in [12]. Furthermore, the Time-of-Flight concept calculates the time it takes for a heat wave to go from the heater to the detector in two specific locations. The benefits of this method include independent data collection regardless of fluid properties, automatic calibration, and multi-parameter measurement. It can also overcome technical obstacles that calorimetric sensors cannot manage [13–14]. One dimensional NTC method is proposed in the literature [6-7]. However, in one-dimensional design, the advantage of the NTC method cannot be utilized efficiently. For this reason, in this study, two-dimensional NTC thermistors are used for the proposed sensor design, and a MATLAB-based simulation of this design is presented in this article. In this simulation, four NTC thermistors are positioned in different orientations (north, south, east, and west) to detect temperature variations caused by wind flow. As the wind cools each thermistor, resistance decreases and the resulting current changes are used to estimate wind speed and direction. A sample of measured temperature values relative to each direction is used in this study. Then, the differences between the calculated and actual wind values are calculated. Finally, the wind direction and wind speed are obtained.

The remainder of this paper is organized as follows: In Section 2, the thermal methods of the wind measurement are given in detail. In Section 3, the proposed method is discussed. The related results are given in Section 4. Section 5 concludes the paper.

## 2. Thermal Methods of Wind Measurement

### 2.1. 2-D Thermal flow sensor

As shown in Figure 1, a square silicon device that combines four resistive heaters, a diode, and thermopiles are used to design a 2-D thermal flow sensor. The temperature of the chip is continuously maintained higher than the airflow temperature by a feedback loop and a central diode [15–16]. The airflow asymmetrically cools the chip, creating a slight temperature gradient. The thermopiles detect this gradient, enabling wind direction and speed to be determined. The gradient's direction corresponds to the flow direction. Meanwhile, its magnitude is approximately proportional to the square root of the flow speed [8-17].

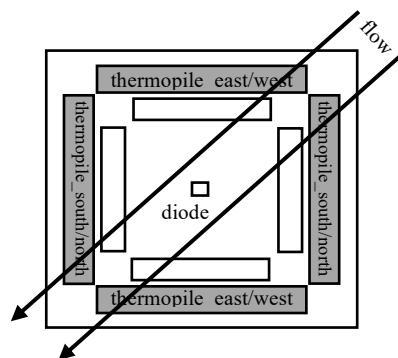


Figure 1. 2-D Thermal Wind Sensor [17].

One aspect of this design is the low-offset instrumentation amplifier that processes microvolt-level signals from thermocouples using a chopper amplifier to reduce noise and thermal offset. The amplifier minimizes thermal offset to 20  $\mu\text{V}$  and provides differential output to reduce common-mode noise.

The system includes wind sensor elements, a multiplexer-connected amplifier, and an analog-to-digital converter (A/D). Tests show accurate results at low wind speeds, with minor deviations at high speeds, and the sensor responds quickly and consistently to wind direction changes [17].

### 2.2. Micromachined 2-D thermal wind sensor

The thermal wind sensor utilizes MEMS (Micro-Electromechanical Systems) technology to monitor temperature differences and heat dissipation caused by wind, enabling precise wind direction and speed measurements. A semi-empirical temperature model compensates for temperature drift using parameters derived from uncompensated output voltage [18–19–20].

The sensor, as shown in Figure 2, consists of eight self-heating thermistors on a ceramic substrate, arranged symmetrically along East-West and North-South axes to form Wheatstone bridges. One bridge maintains steady heater temperature, while the other adjusts for fluid temperature changes. Voltage differences across the bridges indicate wind direction, and terminal voltage measures wind speed [12–21].

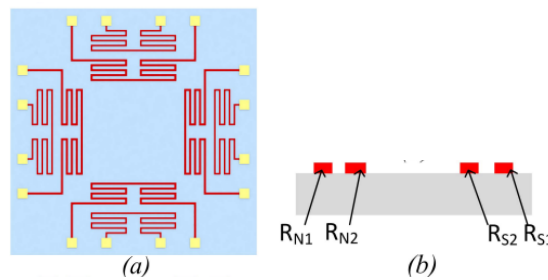


**Figure 2.** (a) Schematic of a thermal wind sensor, (b) a cross-sectional view [22].

In [12], Temperatures between 270 and 310 K and wind speeds between 0 and 40 m/s were tested on the sensor. With measurement errors of less than  $\pm 1.5$  m/s, it was observed that the sensor’s output voltage decreased as the wind speed increased. Testing revealed that the sensor has a weak temperature dependency when measuring wind direction. These findings imply that the sensor performs accurately and sensitively in various conditions [9–12].

In another study, as given in Figure 3 eight heaters and thermistors, divided into two separate wind-sensing groups (cross-type and saltire-type) are included in the design. The sensor averages the data from these two groups to determine the wind direction and speed. This structure aims to decrease heat conduction and increase measurement accuracy [23–24]. In another study, the sensor uses thermistors positioned all around a central heater to measure temperature fluctuations caused by wind [25–26]. The uneven cooling brought on by the wind blowing across the sensor results in a temperature differential on the chip. This variance is used to determine the direction and speed of the wind. To calculate the final wind speed and direction, the sensor averages the data collected from two different wind sensing groups: cross-type and saltire-type.

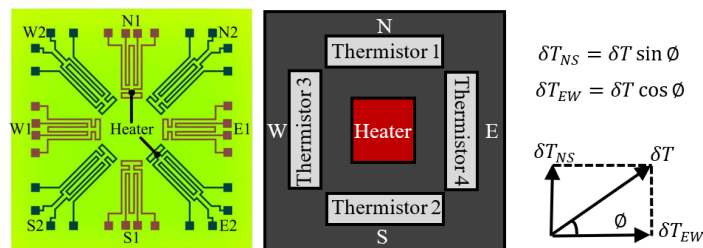


**Figure 3.** The high-accuracy micromachined thermal wind sensor layout. Includes a red cross-type group (N1-E1-S1-W1) and a blue saltire-type group (N2-E2-S2-W2) and its operating principle [24].

The sensor measures wind speed up to 33 m/s with an error of less than 1% and detect wind direction within a 360° range with a maximum error of ±1.5°. The sensor can rapidly and precisely estimate the wind's direction and speed by using measurements from the cross-type and saltire-type groups. Experimental results indicate that this sensor delivers lower error rates when compared to current 2D MEMS thermal wind sensors [24].

### 2.3. NTC Segmented thermistor-based anemometer

The sample structure of the NTC Segmented thermistor-based anemometer is given in Figure 4. The uniaxial anemometer is constructed with a sizable wooden structure and is built utilizing thick-film segmented thermistors with a negative temperature coefficient (NTC). It works based on the variable heat loss in the thermistors as a function of airflow speed. A DC constant voltage causes the thermistors to self-heat, and airflow modifies their resistances. This change is used to determine wind direction and speed. A positive difference indicates that the wind is blowing in one direction, while a negative difference indicates it is blowing in the opposite direction [27-28].

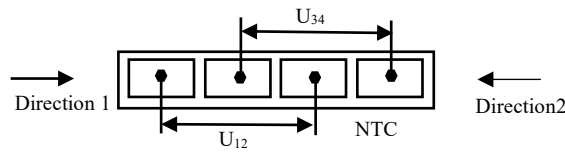


**Figure 4.** The measurements of voltage variances across the sensor's internal electrodes [28].

As shown in Figure 4, the direction of the wind is ascertained by measuring the voltage difference ( $dU$ ) where  $U_{12}$  and  $U_{34}$  denote the measured voltage values. The voltage difference is calculated as given in Equation (1).

$$dU = U_{12} - U_{34} \tag{1}$$

The anemometer underwent testing for wind speeds ranging from 1 m/s to 15 m/s at various inlet air temperatures between -20°C and +40°C. When tested at temperatures above 0°C, delays in the cooling and heating processes were observed at specific intervals, with a determined delay time of 180 seconds (3 minutes) for the anemometer with a 1.6 mm aperture. The measurement sensitivity was confirmed to be accurate within ±3% for wind speed and error-free for wind direction [29-30].

### 2.4. Thermal time-of-flight flow sensor

A Thermal Time-of-Flight (TOF) sensor usually includes one sensing element and one heater. The schematics for the design and the functional block diagram are presented in Figure 5. However, to improve accuracy, it can be designed with three sensing elements. In this configuration, each pair of elements can serve as a TOF sensor. The heater and sensing elements are situated on a thermally insulated membrane.

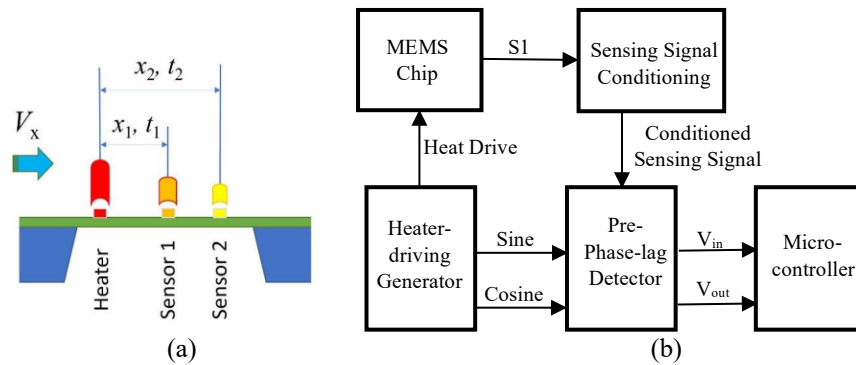


**Figure 5.** (a) Schematic for the thermal TOF wind sensor [13]  
(b) TOF circuit functional block diagram [14].

A single-frequency drive approach is used to measure the phase shift between the heater and sensing element, which is inversely proportional to the flow rate. A heater drive generator excites the heater, a sensing signal conditioner amplifies signals, a Pre-Phase Delay Detector measures phase delay, and a Microprocessor calculates the flow speed based on heat wave travel time.

This method offers high accuracy, noise resistance, and exceptional stability in low flow rate conditions, outperforming other thermal flow sensing technologies in consistency and repeatability [13-14].

### 3. Proposed 2D NTC Based Wind Measurement Method

Based on the research results obtained from the examination of the designs mentioned in the article, a simulation of the NTC (Negative Temperature Coefficient Thermistor) based wind sensor design was performed as shown in Figure 7. In this design, the wind direction and speed are determined using four NTC thermistors. These sensors are placed in the North (0°), East (90°), South (180°), and West (270°) directions; the analog signals from the NTC sensors are converted to digital data via an ADC and sent to the microprocessor. The microprocessor processes this data to detect the impact of wind on temperature and calculate wind speed and direction. Lateral airflow is greatly reduced by the plus (+) shaped housing covering the 4 sensors (W x H = 1 cm x 1 cm).

The NTC thermistors are connected to a constant DC voltage source, allowing it to self-heat, with a measuring range of -40°C to 85°C. The resistance  $R$  of an NTC thermistor decreases with increasing temperature as given in the Equation (2),

$$\frac{1}{T} = A + B \ln(R) + C [\ln(R)]^3 \tag{2}$$

where  $T$  is the temperature in Kelvin,  $R$  is the thermistor resistance, and  $A$ ,  $B$ , and  $C$  are constants derived from measured resistance at different temperatures. Figure 6 shows the temperature-resistance relationship of the NTC thermistor. As the temperature increases, the resistance decreases rapidly.

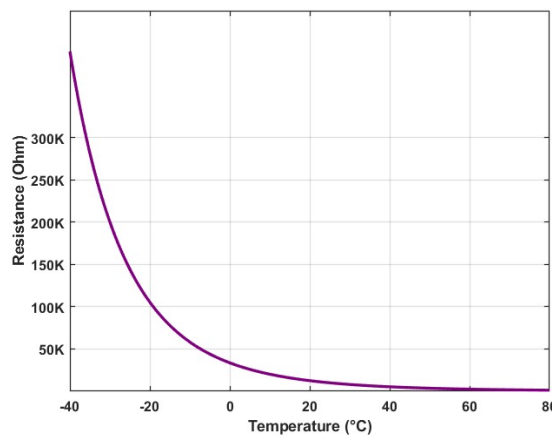


Figure 6. NTC Resistance - Temperature variation.

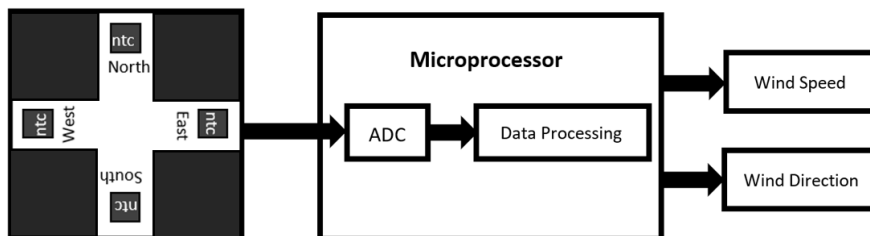


Figure 7. NTC Based wind sensor design.

When wind passes over a thermistor, it cools the thermistor, leading to a decrease in its resistance. As wind speed increases, the thermistor’s resistance decreases further, and the current flowing through it increases accordingly. This behavior allows the estimation of wind speed based on current changes. The thermistor with the highest current among the four directions indicates the primary direction of the wind, providing the most accurate data for determining wind speed.

A simulation for this design was performed using MATLAB. Firstly, test data for different wind speeds (from 0 m/s to 30 m/s) and directions (0°, 90°, 180°, and 270°) are created and environmental parameters such as maximum temperature drop and minimum wind speed are defined. For each combination of wind speed and direction, wind speed and direction estimations are completed using temperature data from the four sensors.

Current values obtained from the NTC thermistor, which is selected for measuring wind direction, are converted to wind speed using a pre-established calibration curve. During calibration, Equation (3) is created based on current values (*a*, *b* and *c*) measured at specific wind speeds where *I* (*T*,*v*) The current (mA) depends on wind speed (*v*) and temperature (*T*)

$$I(T, v) = a(T). \ln (v + b) + c(T) \tag{3}$$

The constants *a*, *b* and *c* are determined through a calibration process; *a* is the temperature dependent sensitivity coefficient, *b* is a constant representing the minimum offset of the velocity and *c* is the temperature dependent offset current. During calibration, the system is tested at known wind speeds, and the corresponding current values are measured for each speed. For example, a current of 1.2 mA is measured at a wind speed of 2 m/s and 3.5 mA at a wind speed of 10 m/s. These values are used to create an equation. These constants are then used throughout the simulation to accurately estimate wind speed from the measured current values.

Wind direction is determined based on the temperature values of the sensors in the four directions. The sensor in the direction of the wind experiences the most cooling and shows the lowest temperature. Thus, the direction of the sensor with the lowest temperature was accepted as the wind direction. For example, if the sensor in the north shows the lowest temperature, it is concluded that the wind is coming from the north.

For each speed and direction combination, the estimated wind speed and direction is compared with the actual (known) values. The error rate between the estimated and actual wind speed is calculated and results for each wind speed and direction combination are recorded in a table. This table includes actual wind speed, actual direction, estimated wind speed and direction, speed and direction error rates, and temperature values for the four directions.

#### 4. Experimental and Simulation Results

During the simulation, the resistance of the NTC sensors varied in response to temperature changes, and this variation was used to calculate wind speed based on the applied formulation. The simulation was conducted for different temperature and wind speed conditions, yielding the following sample results:

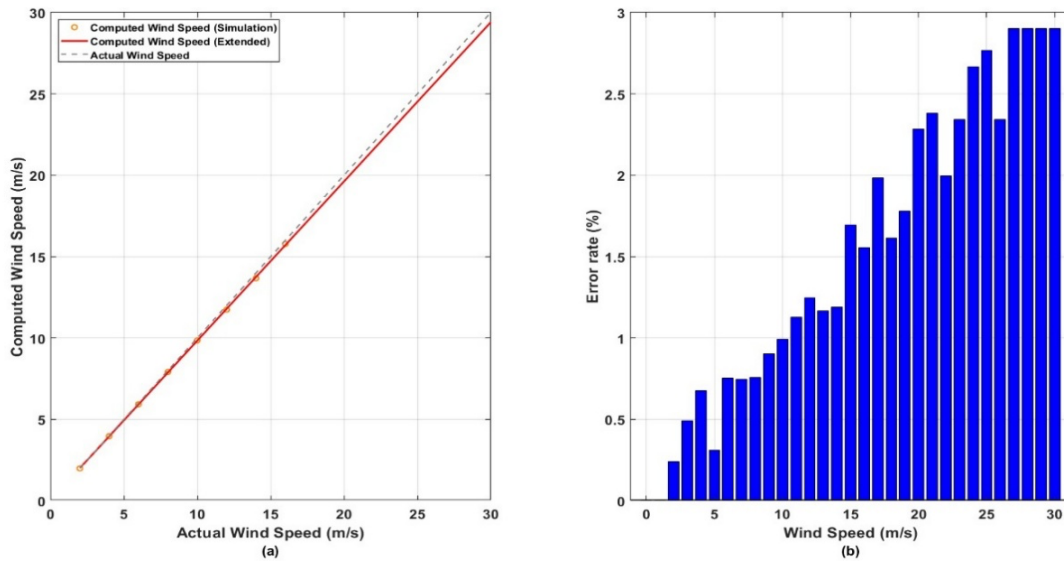
**Table 1.** Sample values and results of the simulation.

Wind Speed (m/s)	Wind Direction (°)	Computed Wind Speed (m/s)	Computed Wind Direction (°)	Wind Speed Error Rate (%)	Temp. (North) (°C)	Temp. (South) (°C)	Temp. (East) (°C)	Temp. (West) (°C)
2	0	1.99	0	0.05	24.54	24.58	25	25.01
4	90	3.97	90	0.75	23.94	23.87	24.01	23.98
6	180	5.93	180	1.14	22	22.37	21.74	22.2
8	270	7.91	270	1.63	20.89	21.01	21	20.61
10	0	9.85	0	1.42	18.54	18.58	19	19.01
12	90	11.74	90	2.14	16.94	16.86	17.1	17.3
14	180	13.67	180	2.32	16	16.01	15.58	16.02
16	270	15.78	270	1.73	14.89	15.01	15	14.61

Figure 8 (a) illustrates the relationship between actual wind speeds (*v<sub>actual</sub>*) and computed wind speeds (*v<sub>computed</sub>*) based on Table 1 using the linear model given in Equation (4);

$$v_{computed} = a. v_{actual} + b = (0.9786). v_{actual} + 0.0479 \tag{4}$$

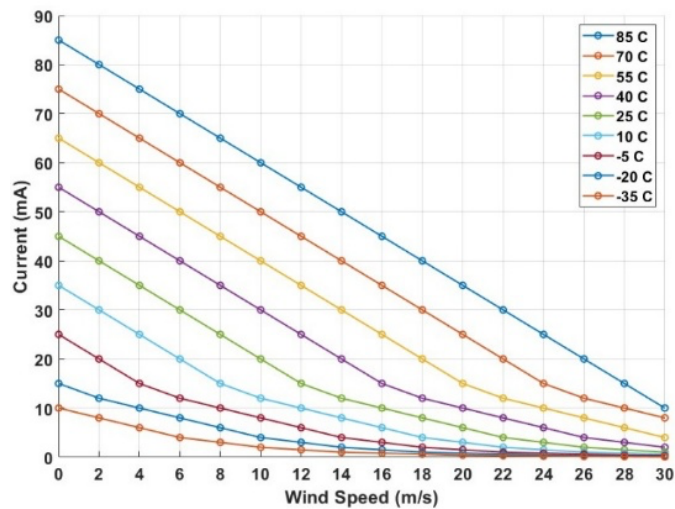
The computed speeds align closely with the ideal line ( $v_{\text{computed}}=v_{\text{actual}}$ ).



**Figure 8.** (a) Simulation results for actual and calculated wind speed measurements, (b) Simulation results for wind speed measurements error rates

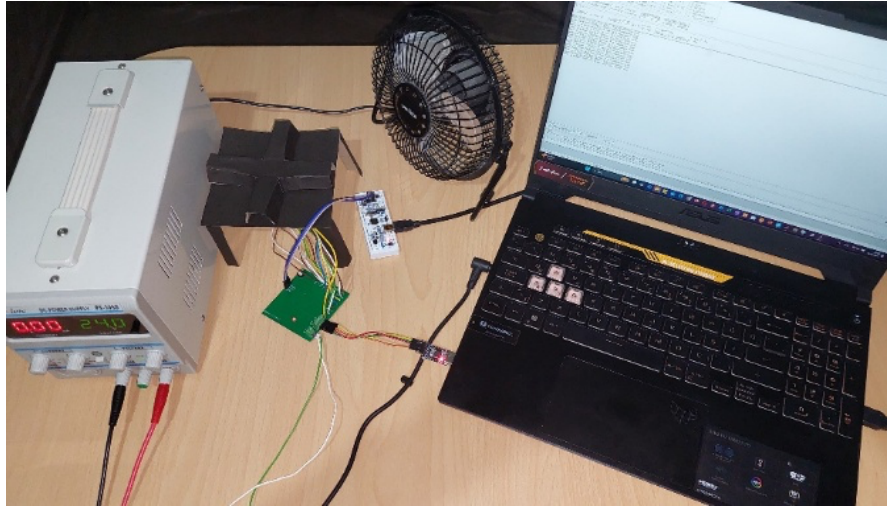
Considering the variations in Figure 8 (a), the orange points represent the computed wind speeds derived from the system, while the red line extends the computed values to higher wind speeds (up to 30 m/s). The dashed gray line represents the ideal relationship where computed and actual speeds are equal. The close alignment of the orange points and the red line with the ideal line demonstrates the system’s accuracy in estimating wind speeds, even at extended ranges. While in Figure 8 (b), the graph highlights the error rates for different wind speeds (1m/s – 30 m/s), represented by blue bars. The error rates remain below 3% across the tested wind speeds, with slight variations. The gradual increase in error rates at higher wind speeds suggests the system maintains reliable performance with only minimal deviations. This consistency reflects the system’s robustness and precision in both low and high wind speed conditions.

Figure 9 shows the relationship between wind speed and current at different temperatures. As wind speed increases, current decreases. At higher temperatures, the current is higher, while at lower temperatures, it is lower. This allows for analyzing the system’s performance based on wind speed and temperature



**Figure 9.** Expected temperature response according to simulation for different temperatures.

Figure 10 shows the test setup of an electronic circuit board, including a power supply, a fan, the circuit board, and a laptop to receive the processed data. The temperature analog data obtained from the 4 NTC thermistors is converted into digital values using the ADC module of the STM32 microcontroller, and then the wind data is processed. The data is transmitted to the computer via the UART protocol using the UART-USB converter.



**Figure 10.** Electronic board and test setup.

The results of the wind direction measurement experiment in Table 2 conducted at a wind speed of 2 m/s, demonstrate that the computed wind direction aligns accurately with the actual wind direction in all instances. The sensor positioned in the direction of the wind consistently records the lowest temperature due to the cooling effect of the wind, with only small temperature differences observed between directions. This highlights effective calibration and reliable performance in detecting wind direction based on temperature variations.

**Table 2.** Sample values and results of the test (at 3 m/s).

Actual Wind Direction (°)	Computed Wind Direction (°)	Temp. (North) (°C)	Temp. (South) (°C)	Temp. (East) (°C)	Temp. (West) (°C)
0	North (0)	24.44	25	24.53	25.21
90	East (90)	24.89	25	24.79	25.21
180	South (180)	25	24.74	25.93	25.19
270	West (270)	24.96	24.83	25.90	24.61

## 5. Discussion

This system’s low cost and straightforward design offer a solution for applications with limited volume. Unlike typical wind sensors, it doesn’t require mechanical components, preventing problems like mechanical wear. Furthermore, NTC sensors are perfect for long-term monitoring applications due to their low energy consumption. More sophisticated algorithms and optimizations can be used to further increase the accuracy of the system. Table 1 summarizes the data obtained from the simulation for different wind speeds and directions. For each test, the actual and calculated wind speed and direction, error rates, and temperature values measured in four directions (north, south, east, west) are presented. The error rate between actual and calculated values generally remained below 3%, indicating that the system operates with high accuracy. According to the table, the sensor in the direction of the wind recorded the lowest temperature, demonstrating the system’s ability to accurately determine wind direction. An experimental method was carried out to validate the system at a wind direction of 25° and a speed of 2 m/s. However, testing for different wind speeds and different temperatures would require higher costs and the procurement of necessary testing equipment. Which may be done in the next step. Table 2 summarizes the data obtained from the experiment for different wind directions. The actual and computed wind directions are

consistent, indicating a low error rate. In each case, the sensor facing the wind recorded the lowest temperature, demonstrating the system's ability to accurately detect wind direction. The results confirm that the system operates with high accuracy and precision. A comparison is also conducted between the proposed design and different sensor designs based on parameters in Table 3.

**Table 3.** Comparison table of the examined sensor designs.

Parameter	2-D Thermal Flow Sensor	MEMS 2-D Thermal Wind Sensor	Octagon-Shaped 2-D Thermal Wind Sensor	NTC Segmented Thermistor-Based Anemometer	Thermal Time-of-Flight (TOF) Flow Sensor	2D NTC-Based Anemometer (proposed work)
Maximum Wind Speed (m/s)	40	40	33	15	30	30
Minimum Wind Speed (m/s)	0	0	0	1	0	1
Error Rate (%)	±3	±2 Speed ±3 Direction	±1 Speed ±1.5 Direction	±3	±2.5	±3

Some positive and negative aspects of all methods are discussed here. The 2-D Thermal Flow Sensor is compact with high sensitivity but struggles at low temperatures and power efficiency. The MEMS 2-D Thermal Wind Sensor offers precision via a double Wheatstone bridge but may face instability at high wind speeds. The Octagon-Shaped 2-D Sensor ensures real-time accuracy but has complex packaging challenges. The NTC Segmented Anemometer is low-cost and simple but experiences heating and cooling delays. The TOF Flow Sensor is reliable and sensitive but affected by humidity. The proposed 2D NTC-Based Anemometer is energy-efficient and cost-effective but may have thermal response delays.

## 6. Conclusion

Thermal-based flow sensors provide high sensitivity, accuracy, and energy efficiency. However, there is room for improvement in thermal insulation design to enhance its performance at low temperatures. Data obtained using the phase delay detection method showed stability in low flow rate ranges compared to other thermal flow sensing technologies, which experienced significant fluctuations. Implementing new modulation techniques and low-power consumption circuits can help reduce energy consumption. Furthermore, advanced calibration techniques can be developed for more accurate measurements under different environmental conditions. In this study, different thermal flow sensor designs reported in the literature are reviewed, and a novel method based on 2 dimensional NTC sensor is proposed. The sensor operated with a delay of 2-3 minutes at 25°C. During the experiments, wind speed was measured between 1 m/s and 16 m/s, and the minimum measured wind speed was determined as 1 m/s. According to the results, actual and calculated wind speed measurements are well matched, and the maximum wind speed error observed is less than %3. Looking ahead, there is a need for these sensors to be designed to perform reliably over a wider temperature range and be suitable for use in various application areas. New modulation techniques and low-power consumption circuits could be utilized to increase the efficiency. Environmental factors significantly impact the performance of the anemometer, such as temperature, humidity, and heat loss. Temperature variations affect thermistor sensitivity, while heat loss impacts accuracy, particularly at lower temperatures. Design improvements, such as better thermal insulation and optimized thermistor materials, are suggested to enhance performance in extreme conditions.

## References

- [1] Aleksic SO, Mitrovic NS, Nikolic Z, Lukovic MD, Obradovic NN, Lukovic S. G. Three-Axis' Heat Loss Anemometer Comprising Thick-Film Segmented Thermistors. *IEEE Sens J* 2019; 19 (22): 10228-10235.
- [2] Gutarra JS, Gastelo-Roque JA, Sulluchuco J. A cup anemometer using 3D additive manufacturing. 2020 IEEE 27th Int. Conf. Electron Electr Eng Comput (INTERCON); 03-05 September 2020; Lima, Peru.
- [3] Perez del Valle, M, Urbano Castelan JA, Matsumoto Y, Cortes Mateos R. Low Cost Ultrasonic Anemometer. 2007 4th Int Conf Electr Electron Eng (ICEEE); 05-07 September 2007; Mexico City, Mexico. 213-216.
- [4] Le Duff A, Plantier G, Gazengel B. Real-Time Particle Detection and Velocity Measurement by Means of Laser Doppler Velocimetry. 2005 IEEE Instrum Meas Technol Conf (IMTC); 16-19 May 2005; Ottawa, ON, Canada. 2222-2225.
- [5] Chen J, Liu C. Development and characterization of surface micromachined, out-of-plane hot-wire anemometer. *J Microelectromech Syst* 2003; 12 (6): 979-988.

- [6] Wang, S, Yi Z, Qin M, Huang QA. Temperature effects of a ceramic mems thermal wind sensor based on a temperature-balanced mode. *IEEE Sens J* 2019; 19 (17): 7254–7260.
- [7] Zhu Y, Qin M, Huang J, Yi Z, Huang Q. Sensitivity Improvement of a 2D MEMS Thermal Wind Sensor for Low-Power Applications. *IEEE Sens J* 2016; 16 (11): 4300-4308.
- [8] Makinwa KAA, Huijsing JH. A wind-sensor interface using thermal sigma-delta modulation techniques. *Sens Actuators A Phys* 2001; 92 (1-3): 280-285.
- [9] Sosna C, Buchner R, Lang W. A temperature compensation circuit for thermal flow sensors operated in constant-temperature-difference mode. *IEEE Trans Instrum Meas* 2010; 59 (6), 1715–1721.
- [10] Que RY, Zhu R, Que QZ, Cao Z. Temperature compensation for thermal anemometers using temperature sensors independent of flow sensors. *Meas Sci Technol* 2011; 22.
- [11] Nguyen NT, Kiehnscherf R. Low-cost silicon sensors for mass flow measurement of liquids and gases. *Sens Actuators A Phys* 1995; 49 (1-2): 17-20.
- [12] Gao S, Yi Z, Ye Y, Qin M, Huang QA. Temperature Effect and Its Compensation of a Micromachined 2-D Anemometer. *IEEE Sens J* 2019; 19 (14): 5454–5459.
- [13] Huang L. Micromachined Thermal Time-of-Flight Flow Sensors and Their Applications. *Micromachines* (Basel). 2022; 13 (10): 1729.
- [14] Yao Y, Chen C, Wu X, Huang L. MEMS Thermal Time-of-Flight Flow Meter. 15th Flow Meas Conf (FLOMEKO); 13-15 October 2010; Taipei, Taiwan.
- [15] Matova SP, Makinwa KAA, Huijsing JH. Compensation of Packaging Asymmetry in a 2-D Wind Sensor. *IEEE SENSORS* 2002; 12-14 June 2002; Orlando, FL, USA. 1256-1259.
- [16] Nam T, Kim S, Park S. The temperature compensation of a thermal flow sensor by changing the slope and the ratio of resistances. *Sens Actuators A Phys* 2004; 114 (2-3): 212-218.
- [17] Makinwa KAA, Huijsing JH. A wind sensor with an integrated low-offset instrumentation amplifier. 2001 8th IEEE Int Conf Electron., Circuits Syst (ICECS); 02-05 September 2001; Malta, Malta. 1505-1508.
- [18] Van Putten AFP, Van Putten MJAM, Van Putten MHPM. Silicon thermal anemometry: developments and applications. *Meas Sci Technol* 1996; 7: 1360-1377.
- [19] Yi Z, Ye Y, Qin M, Huang Q. Modeling of Packaged MEMS Thermal Wind Sensor Operating on CP Mode. *IEEE Trans Electron Devices* 2019; 66 (5): 2375-2381.
- [20] Kim S, Nam T, Park S. Measurement of flow direction and velocity using a micromachined flow sensor. *Sens Actuators A Phys* 2004; 114 (2-3): 312-318.
- [21] Que RY, Zhu R, Wei QZ, Cao Z. Temperature compensation for thermal anemometers using temperature sensors independent of flow sensors. *Meas Sci Technol* 2011; 22.
- [22] Gao S, Yi Z, Ye Y, Qin M, Huang QA. Configuration of a Self-Heated Double Wheatstone Bridge for 2-D Wind Sensors. *J Microelectromech Syst* 2018; 28 (1): 125-130.
- [23] Dong Z, Huang Q, Qin M. Thermal Asymmetry Compensation of a Wind Sensor Fabricated on Ceramic Substrate. *IEEE SENSORS* 2010; 01-04 November 2010; Waikoloa, HI, USA. 595-599.
- [24] Ye Y, Yi Z, Gao S, Qin M, Huang Q. Octagon-Shaped 2-D Micromachined Thermal Wind Sensor for High-Accurate Applications. *J Microelectromech Syst* 2018; 27 (4): 739-747.
- [25] Chen B, Zhu Y, Qin M, Huang Q. Effects of Ambient Humidity on a Micromachined Silicon Thermal Wind Sensor. *J Microelectromech Syst* 2014; 23 (2): 253-255.
- [26] Dong Z, Chen J, Qin Y, Qin M, Huang Q. Fabrication of a Micromachined Two-Dimensional Wind Sensor by Au–Au Wafer Bonding Technology. *J. Microelectromech. Syst* 2012; 21 (2): 467-475.
- [27] Fritsch S, Sarrias J, Brieu M, Couderc JJ, Baudour JL, Snoeck E, Rousset A. Correlation between the structure, the microstructure and the electrical properties of nickel manganite negative temperature coefficient (NTC) thermistors. *Solid State Ion* 1998; 109 (3-4): 229-237.
- [28] Aleksic OS, Maric VD, Zivanov LD, Menicanin AB, A Novel Approach to Modeling and Simulation of NTC Thick-Film Segmented Thermistors for Sensor Applications. *IEEE Sens J* 2007; 7 (10): 1420-1428.
- [29] Menicanin AB, Aleksic OS, Nikolic MV, Savic SM, Radojic BM. Novel Uniaxial Anemometer Containing NTC Thick Film Segmented Thermistors. 2008 26th Int Conf Microelectron (MIEL); 11-14 May 2008; Nis, Serbia and Montenegro.
- [30] Aleksic O, Radojic B, RamovicR. Electrode Effect on NTC Planar Thermistor Volume Resistivity. 2006 25th Int Conf Microelectron (MIEL); 14-17 May 2006; Belgrade, Serbia.